

PREPARATION AND CHARACTERIZATION OF SLAG REINFORCED TOUGHENED EPOXY COMPOSITES

Ahmad Mousa¹, Michaela Gedan-Smolka², Kornelia Schlenstedt²

¹Department of Materials Engineering, Faculty of Engineering
Al-Balqa Applied University, Salt 19117 Jordan, mousa@rocketmail.com, mousa1@bau.edu.jo (A.M.)

²Leibniz-Institut für Polymerforschung Dresden e. V.
Hohe Strasse 6, D-01069 Dresden
Germany, mgedan@ipfdd.de (M.S.); schlenstedt@ipfdd.de (K.S.)

Received 20 June 2024

Accepted 08 September 2024

DOI: 10.59957/jctm.v60.i1.2025.11

ABSTRACT

The current investigation reports the influence of siliconized slag powder on the mechanical properties of epoxy composites. At first, the received slag was crushed and milled followed by sieve analysis. The chemical composition of the slag waste of the steel-making process was inspected using X-ray fluorescence spectroscopy (XRF). Second, the treated slag was mixed with silicone rubber at high speed to produce siliconized slag. Then slag with and without silicon was incorporated into epoxy resin to produce epoxy composites, and mixing was done at the high-speed mixer. The mix was poured into Teflon-coated molds and allowed to harden for 3 days at room temperature. The mechanical performance of the prepared composites was inspected. Chemical functional groups and molecular structure were analysed with attenuated total reflectance infrared spectroscopy (ATR-IR). The samples were examined with a Scanning electron microscope associated with energy-dispersive X-ray spectroscopy (SEM/EDX). Such a technique was used to obtain an idea of the fracture mode and the dispersion pattern of slag powder within the matrix and the chemical composition of the slag.

Keywords: silicon rubber, slag, re-use, sustainability, strength, composition.

INTRODUCTION

Slag can be defined as a by-product during the processing of both ferrous steel and iron blast furnaces. Currently, the amount of slag deposited as a landfill material leads to serious pollution to the environment. To minimize this issue slag utilization is an important way to get rid of such problems. The physical and chemical characteristics of steel slag trigger its utilization in various industrial applications such as steel enterprise, road asphalt, cement and concrete additive, and construction materials for civil applications [1 -3]. It has been found that the major composition of ferrous slag is calcium and silicone. Steel slag may contain significant iron amounts, whereas magnesium and aluminium may be significant in ferrous slag. Note that oxides are the most reported major components in

ferrous slag. Based on the literature it has been found that slag has been utilized in construction material or as a secondary metal resource during extraction and in environmental remediation applications [4 -7].

In this regard i.e. environmental applications non-ferrous slag has been used more than ferrous slag as reported in the literature. However, for ferrous slag, the reported studies have focused on the characterization of the physical properties and applications of slag as a waste material. Ferrous slag is commonly alkaline due to the presence of calcium silicates, carbonates, and oxides, which in some applications is a favourable attribute [8 -10]. To the best of the author's knowledge, the application of slag waste as a potential reinforcing agent into epoxy resin is not well reported. It may be known that the inorganic nature of the slag could limit its performance with organic polymers [11 - 13].

This work aims to incorporate raw and modified slag waste material within the epoxy resin to produce slag-based composite material. The aim of this is to improve the performance of the epoxy composite material. Therefore, dual advantages will be obtained the first is economical and the latter is ecological by avoiding dumping the slag as landfill material.

EXPERIMENTAL

Materials and methods

Commercial-grade epoxy resin and hardener were purchased from the local market, (Amman-Jordan), slag was donated from Almanaseer steel factory-Jordan, and commercial-grade silicone rubber paste was purchased from Jordan.

Slag pre-treatment

The received slag powder was subject to two step-by-step comminution processes to break down the size. The first stage was done on a roll crusher model AF32A. to obtain the coarse size. The second stage was done with a ceramic ball mill model (US STONEWARE EAST PALSINE, OH 44413). Milling was done for 16 h at 320 rev. min⁻¹. The milled powder was sifted with an electrical shaker Retsch AS 200 for 10 min. The slag portion with particle size $\leq 100 \mu\text{m}$ was used for the sample preparation during this work. The chemical composition of the slag is presented in Table 1 as detected by XRF and EDX. The density of the slag powder was determined by Helium pycnometer (Ultrapycnometer 1000 T) according to Archimedes' principle [14].

Composite Preparation

The slag was mixed with silicone rubber paste using a high-speed mixer for a few minutes at room temperature to obtain a siliconized slag paste. The paste was kept in a separate container before incorporating into an epoxy composite. The epoxy-reinforced samples were fabricated based on 80:20 wt.% epoxy to slag. The hardener was a polyamide, the ratio of hardener to polymer was 0.5:1 wt.%. The slag and the epoxy resin were thoroughly mixed using an electrical high-speed mixer for a few minutes.

The mix was poured into a mold coated with Teflon. The mix was left to cure at room temperature for 3 days.

The samples were designated in the following manner: the plain epoxy control sample was named "E". The epoxy-containing slag was named "ES", the epoxy with the siliconized slag was "ESiS" and the sample containing silicone rubber was named "ESi"

Tensile strength

Tensile strength at break was performed according to ASTM D-638 by a Zwick 1456 universal tensile testing machine at room temperature. Dog bone-shaped specimens 3 mm thick were tested at a crosshead speed of 2 mm min⁻¹. Three samples were tested, and the average value was reported.

Impact strength

The impact test was done according to ASTM, D-356-88 by CEAST impact tester model 6545. The testing conditions were set as hammer energy was 7.5 J at a speed of 3.0 m s⁻¹.

Hardness

Circular discs with 3 mm thickness were tested on a Zwick 3140 shore D hardness tester according to DIN EN ISO 868.

ATR-IR analysis

The ATR-IR spectra of the samples were directly recorded on a Bruker ATR-IR spectrometer in the transmittance mode in the 400 - 4000 cm⁻¹ region.

SEM-EDX

The impact fractured samples of the composites were examined by SEM-EDX for microstructure and chemical composition analysis with an electron-optical magnification range of 40x to 1000 x and a resolution higher than 1 μm . Excitation voltages of 3 keV for SEM and 12 Kev for SEM-EDX were applied. The SEM Gemini Ultra plus (Zeiss, Germany) with EDX-detector Flat Quad XFlash 5060F (Bruker, United States) was used to run the SEM/EDX experiments. Prior testing samples were coated with 3 nm Pt.

RESULTS AND DISCUSSION

Slag composition

Slag composition was analysed by XRF and SEM-EDX. The results obtained by XRF were confirmed

by the EDS unit of the scanning electron microscope (Table 1).

To analyse the chemical composition of the applied slag, EDX mappings and corresponding sum spectra were acquired at 3 different sample areas of slag in epoxy. The spectra were analysed with the Esprit software (Bruker) using the oxide method with deconvolution of Pt (sample coating prior the SEM-examination) and C (main component of the epoxy matrix). This procedure allows to analyse the slag composition. Observed main elements of the slag are Fe, Ca, Si and Al. In addition, slag contains small amounts of Mg, Mn, Ti, Cr, S and Cl. From EDX-data in Table 1 it is obvious, that slag particles are not homogeneous in chemical composition. Hereafter, the average stoichiometric composition by SEM-EDX is in fair agreement with the XRF data.

Stress-Strain curves.

The related tensile properties of the epoxy composites are depicted in Figs. 1 - 4, consequently. Fig. 1 depicts the load-extension responses of the epoxy composites with different compositions. The ES sample displayed less extension compared to all formulas; this could be due to the increased rigidity of the epoxy composite because of slag functionality. Referring to the sample ESiS, the addition of ESiS has tremendously increased the extensibility (elongation) of the epoxy as reflected by Fig. 1. Hence the conclusion is that the toughness of the composite has been improved as such due to the plasticization role of the siliconized slag.

Tensile properties

Fig. 2 illustrates the tensile strength at break of the various compositions of the epoxy samples. Note that the incorporation of as received slag powder has reduced the tensile strength of the composite with reference to the control. Observe that the ESSi sample showed higher tensile strength as compared to both ES and ESi. The plausible explanation of such finding is due to the dipole-dipole interaction between the epoxy resin and the slag with and without silicon rubber. The dipole-dipole interactions are evidenced by the FTIR spectra displayed in Fig. 3.

The remarkable hint is the sample with pristine slag displayed the highest intense peak detected at 3400 cm⁻¹

Table 1. Slag average chemical composition [%] by XRF and SEM-EDX.

| Component | XRF | SEM-EDX |
|--------------------------------|--------|---------|
| Fe ₂ O ₃ | 28 | 31.8 |
| Al ₂ O ₃ | 13 | 8.3 |
| CaO | 31 | 34.9 |
| SiO ₂ | 19 | 14.3 |
| MnO, MgO and other oxides | traces | traces |

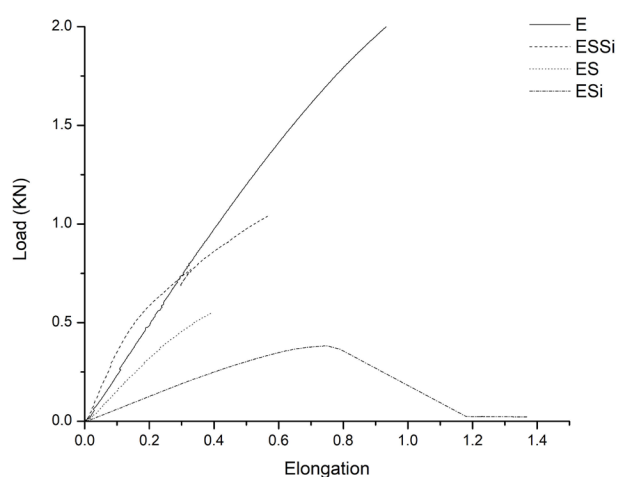


Fig. 1. Stress-Strain curves of Epoxy/slag composites.

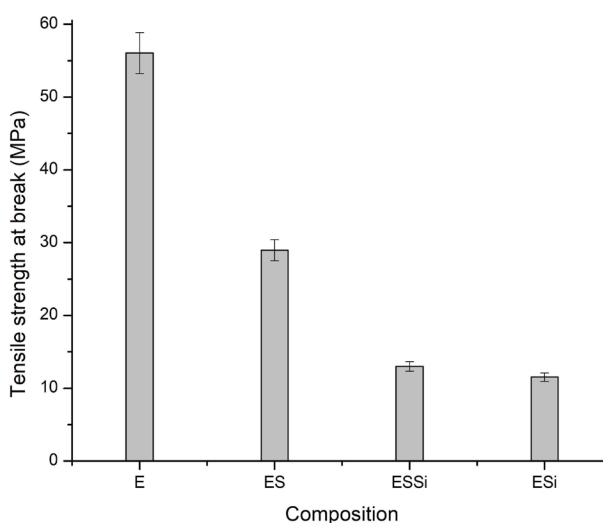


Fig. 2. The effect of S and Si on the tensile strength at break of epoxy composites.

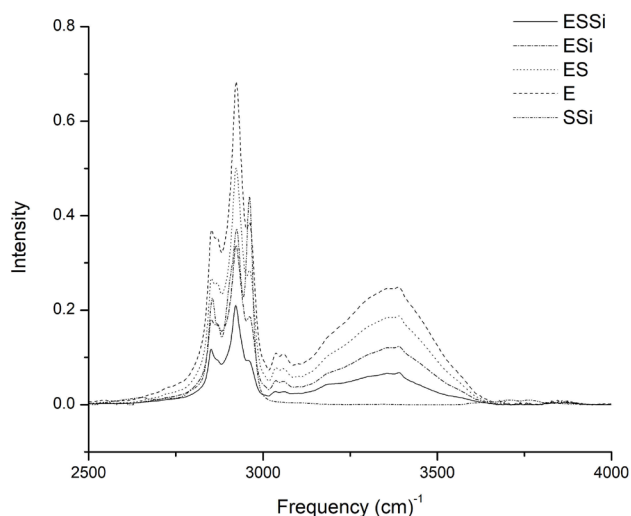


Fig. 3. ATR-IR spectra of siliconized and non-siliconized epoxy composites.

¹. which has been related to the –OH. This is evidence on the curing of the epoxy composite. The increment in the intensity of such peak indicates the high degree of conversion for epoxy as compared to epoxy containing either silicon rubber or siliconized slag. This is in line with a previous work on the relation between the epoxy resin curing and the mechanical properties of the composite reinforced with Aramid/Glass [15].

Simultaneously Fig. 4 shows the elastic Young's modulus of the epoxy composites with S and SSI. The trend displayed here is at odds with the trend found for tensile strength. Note that ES sample has displayed the highest modulus value among all studied samples. The highest modulus value indicates improved stiffness of the ES formula. This is due to the rigidity of the slag powder being conferred to the whole composite.

The lower modulus for the siliconized epoxy sample confirms the plasticizing role of the silicon added to the formula as mentioned earlier. Similar results were recorded in the case of activated slag as an additive to rubberized unsaturated polyester composite: Thermal and mechanical study [16]. The role of unmodified slag and siliconized slag on the EB of all composites is shown in Fig. 5. Note that the ESI formula has significant increment in the EB as compared to the epoxy with and without slag. Such observation should be related to the plasticization role of silicone rubber incorporated with the formula as

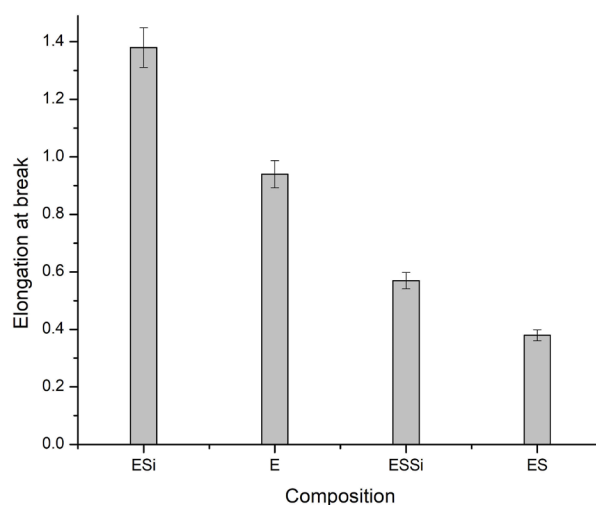


Fig. 4. The effect of S and SSI on the modulus of Epoxy composites.

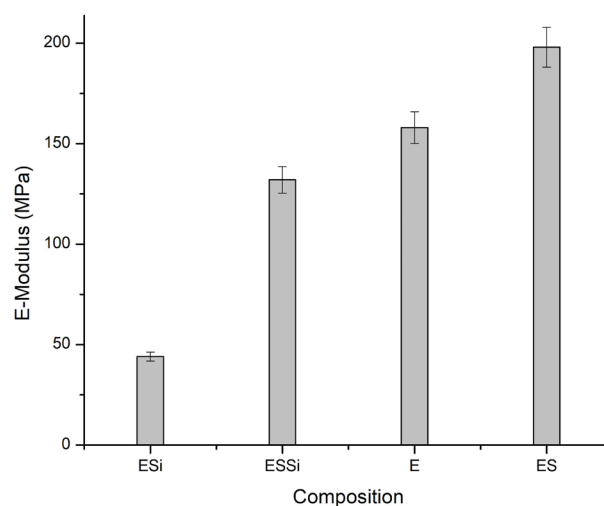


Fig. 5. EB of various formulas of epoxy composites.

mentioned in the previous section. This is in harmony with a previous investigation on the plasticization role of rubber in rigid PVC formulas [17]. Contrary to this, the decreased EB of the ES sample should be related to the rigid nature of the inorganic slag particles which confers rigidity to the sample as well, hence reduced EB is recorded. At the same time the formula with siliconized slag displayed higher EB than the ES formula. This is due to the coating of the slag with silicone layers. Hence better interaction with the matrix consequently higher EB is detected.

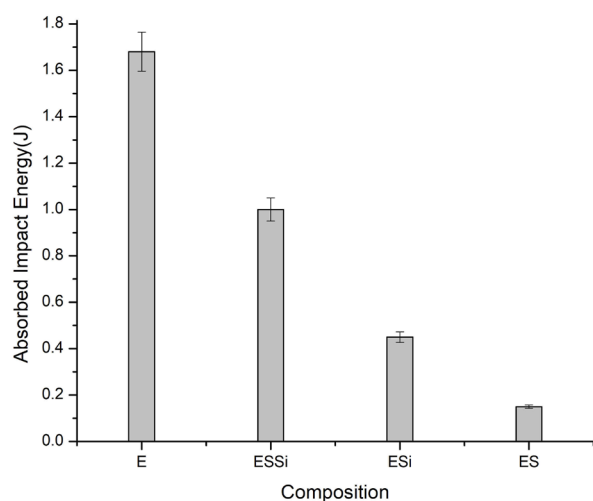


Fig. 6. Impact resistance of epoxy composites with various formulations.

Fig. 6 reflects the un-notched Izod impact resistance of the epoxy composites with different formulas. Note that the siliconized slag containing formula displayed the highest impact resistance compared to the other filled compositions. This agrees with the EB trend reported earlier in the previous section which agrees quite well with a report on plasticized epoxy composite by castor oil [18].

The hardness of the epoxy samples containing various additives are presented in Fig. 7. It is found that the slag containing sample obtained the highest hardness value whereas the sample with siliconized slag displayed the lowest value. The trend here is attributable to the lubrication role of the siliconized slag. Recall that hardness is a toughness related property. The implication is that the sample with the silicon rubber is more ductile which is harmony with the EB and the impact behaviour elaborated earlier.

SEM-EDX analysis of unfilled epoxy and silicon polymers

Fractured surfaces of the prepared epoxy composites containing pristine slag, siliconized slag and toughened composites were examined under SEM-EDX technique to evaluate dispersion pattern of the filler within the matrix and the fracture mode and their content.

Fig. 8 displays the EDX spectra of all prepared

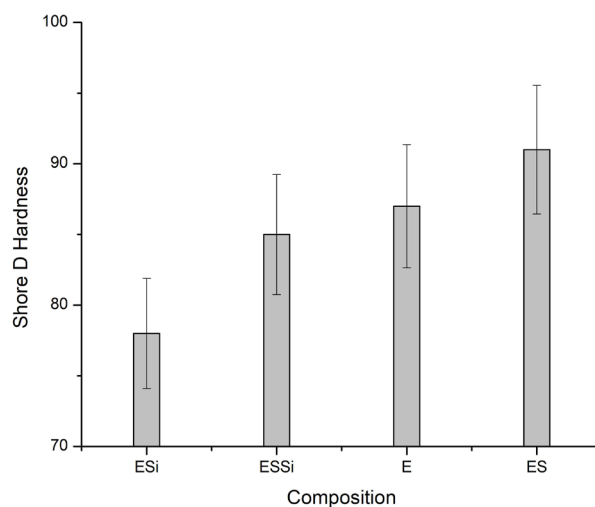


Fig. 7. Shore D hardness of epoxy composites with various structures.

samples in this work. Plain epoxy showed signals for C and O, thus highlighting the organic nature of the cured epoxy. Further the spectra of the silicon rubber showed peaks at Si-, O- and C-energy lines which is related to silicone rubber content. The spectra of the epoxy sample containing slag showed the main elements of slag which are Ca, Si, Fe and Al raised by the slag while the C band is related to the epoxy matrix. Furthermore, minor signals for Mg, S, Cl, Ti, Cr and Mn were recorded as well.

Oxides of these elements are minor components of the slag, as evidenced by XRF-analysis. As expected, the EDX-spectrum of toughened epoxy matrix shows signals for C, O and Si. At last, the sample with siliconized slag displayed a decreased signals for Al, Ca and Fe of the slag compared to the spectrum of the sample with un-siliconized slag. Hence, the Si-signal increased compared to the Si-signal in spectra of silicon or slag in epoxy. This a hint of that a silicone layer was deposited on the slag powder.

SEM-EDX of epoxy composites

The SEM images presented in Fig. 9 illustrate the distribution of the unmodified slag within the epoxy matrix. The slag particles smaller than 5 μm are seen at the sample surface. Particles about 5 - 20 μm were detected in the middle of the sample and large slag particles are at the bottom. The conclusion is that the

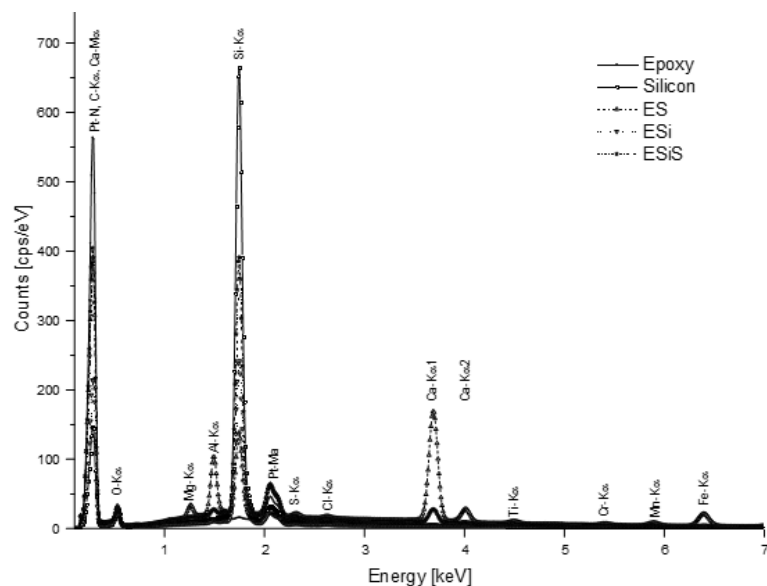


Fig. 8. SEM-EDX-spectra acquired at 12 keV of pure epoxy, silicon rubber, fractured composite surfaces of ES, ESi and ESiS.

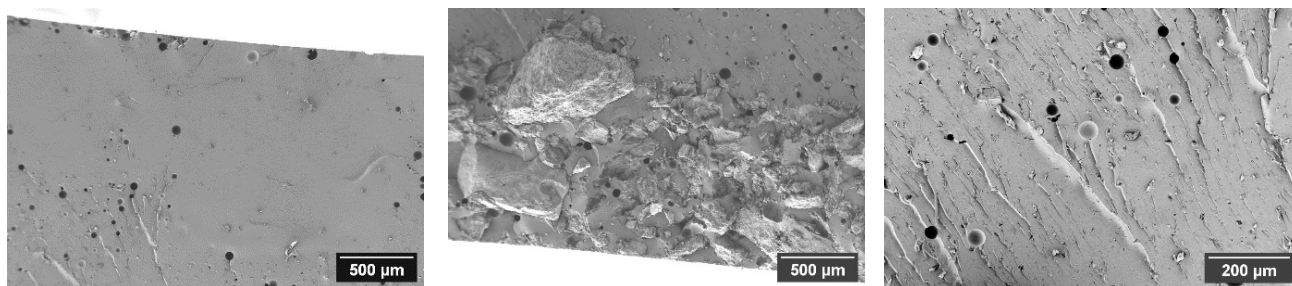


Fig. 9. SEM-images of the fractured cross-section of epoxy with slag, side 1 (left) middle of the fractured area (middle), side 2 of the fractured surface (right).

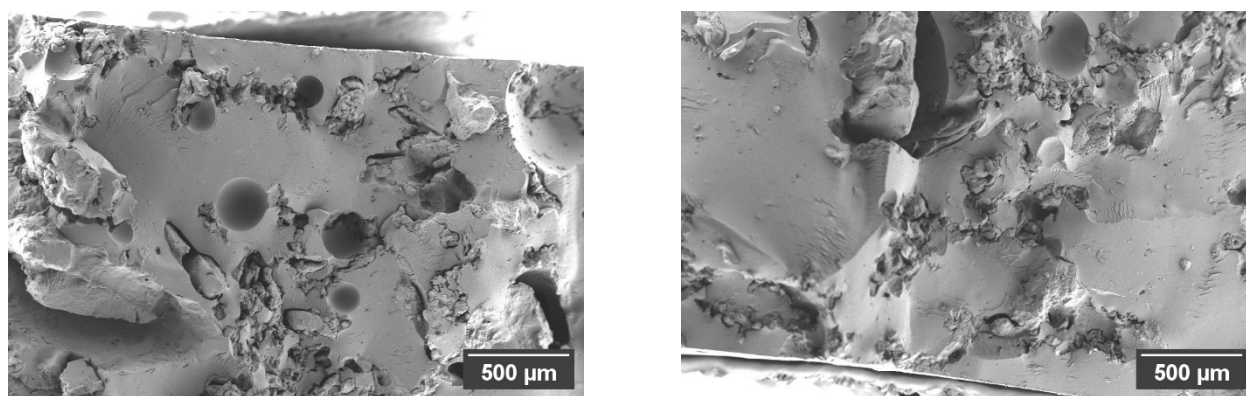


Fig. 10. SEM-images of the fractured cross section of epoxy with slag and siliconized slag, side 1 (left), side 2 of the fractured surface (right).

distribution of the slag is very inhomogeneous where the heavier slag particles are settled at the sample bottom. So, it should be advantageous to remove the

larger particle fraction e.g. by sieving or further milling to get a more homogeneous composite in future.

Fig. 10 displays the SEM images of the fractured

sample for epoxy containing siliconized slag. Both images show rather a ductile fracture mode of the epoxy matrix. This simply indicates that the slag is coated with silicon hence highlighting an improved degree of interaction between the coated slag and the epoxy matrix thus, a successful coating process. Similar trends of slag coated with liquid nitrile butadiene rubber were reported as well [19].

CONCLUSIONS

Based on the results, it is possible to produce composites with scrap material such as slag. The incorporation of slag increased the stiffness of the compounds as indicated by Young's modulus. Further, the incorporation of siliconized slag has improved the toughness as indicated by the elongation at the break of the epoxy samples. Enhancement of the stiffness of the samples has been achieved as indicated by the modulus of elasticity. SEM/EDX studies revealed a successful coating process of the slag with the silicon. Further, the SEM/EDX analysis revealed an inhomogeneous structure of the composites.

The EDX analysis of the slag was in harmony with the XRF results explained earlier. Further classification of the slag particles and selective removal of oversize particles should allow a more homogeneous distribution in the epoxy matrix, avoid sedimentation during the curing, and crack initiation of large slag particles during impact. It is expected that this will lead to further improvement of the mechanical properties of the composite and increase the performance of the reinforcement. Finally, the study has shown that slag waste use supports avoiding landfilling in the future.

Acknowledgments

Prof. Dr. Ahmad Mousa would like to acknowledge the Alexander von Humboldt Foundation for the digital cooperation scholarship to run this work.

Authors' contributions: A.M. designs the formula, prepare the samples and analyse all the data while M.G. contribute to the analysis of the data and revise the manuscript. K.S. did the SEM and EDX images and contributed to the analysis of the EDX spectra.

REFERENCES

1. U.A. Shakil and S.B. Hassan, Behavior and properties of tin slag polyester polymer concrete confined with FRP composites under compression, *J. Mech. Behav. of Mat.*, 29, 2020, 44-56.
2. L.V. Yigang, W. Cui, H. Weiwei, L. Xing, P. Hui, Study of the Mechanical Properties and Microstructure of Alkali-Activated Fly Ash-Slag Composite Cementitious Materials, *Polymers*, 15, 2023, 1903.
3. P. Lohiyaa, A.B. Agrawal, A. Agrawal, A.K. Jain, Thermal Behavior of Epoxy Composites Filled with Micro-sized LD Slag Particulates, *Jord. J. Mech. Indus. Eng.*, 17, 2023, 645-651.
4. A. Mousa, M. Gedan-Smolka, Modification of Mineral Powder by Various Organic Materials: Their Potential as Reinforcement for Unsaturated Polyester Composites., *Russ. J. Appl. Chem.*, 93, 2020, 1968-1975.
5. N.V.K. Prasad, K. Suresh, K. Prasad, Evaluation of Mechanical Properties of Slag Reinforced Polymer Composite, *Intern. J. of Innov. Eng. Technol.*, 4, 2014, 69-78.
6. D. Andjelkovic, A. Culkin, R. Loza, Unsaturated polyester resins derived from renewable resources, *Composites and Polycon*, American Composites Manufacturers Association, 2009, 15-17.
7. L. Ravindran, M.S. Sreekala, S. Anil Kumar, S. Thomas, A comprehensive review on phenol-formaldehyde resin-based composites and foams, *Polym. Compos.*, 43, 2022, 8602-8621.
8. R. Sinha, *Outlines of polymer technology*. Prentice-Hall by India Private Ltd, New Delhi, 2000, 10001.
9. N.M. Nurazzi, A. Khalina, S.M. Sapuan, A.M. Laila, M. Rahmah, Curing behavior of unsaturated polyester resin and interfacial shear stress of sugar palm fiber, *J. Mech. Eng. Sci.*, 11, 2017, 2650-2564,
10. L. Kriskova, L. Machiels, Y. Pontike, Inorganic Polymers from a Plasma Converter Slag: Effect of Activating Solution on Microstructure and Properties, *J. Sustain. Metall.*, 1, 2015, 240-251
11. Y. Pontikes, L. Machiels, S. Onisei, L. Pandelaers, D. Geysen, P.T. Jones, B. Blanpain, Slags with a high Al and Fe content as precursors for inorganic polymers, *Appl. Clay Sci.*, 73, 2013, 93-102.
12. A. Mousa, G. Heinrich, U. Wagenknecht, Toughened

- Unsaturated Polyester Composites Reinforced with Slag Material, *Polym. Plast. Technol. Eng.*, 56, 2017, 1657-1664.
13. A. Mousa, The Effect of feldspar and Kaoline on Mechanical performance of SBR/LDPE composites, *Int. J. Indus. Chem.*, 4, 2013, 26.
14. A. Mousa, G. Heinrich, F. Simon, U. Wagenknecht, KW, Stöckelhuber, Carboxylated Nitrile Butadiene Rubber/Hybrid Filler Composites, *Mat. Res.*, 15, 2012, 671-678.
15. S.L. Valença, E.M Sussuchi, S. Griza, GO Valença, C.P. Santos, Relation between the Epoxy Resin Curing and the Mechanical Properties of the Composite Reinforced with Aramid/Glass, *Res. Soc. and Dev.*, 10, 2021, 23-37.
16. A. Mousa, M. Gedan-Smolka, U. Wagenknecht, Activated slag as an additive to rubberized unsaturated polyester composite: Thermal and mechanical study *J. Vinyl. Add. Technol.*, 26, 2020, 173-179.
17. J.K. Kocsis, J. Gremmels, A. Mousa, U.S. Ishiaku, Z.A Mohd Ishak, Application of hygrothermally decomposed polyurethane in rubber recipes: Part 1.: Natural rubber (NR) and nitrile rubber (NBR) stocks, *Kaut. Gum., Kunst.*, 53, 2000, 528-533.
18. A. Mousa, M. Gedan-Smolka, Epoxy bio composites-based chemically treated coffee dystrophy and castor oil, *Polym. Ren. Res.*, 14, 2023, 31-43.
19. A. Mousa, M. Gedan-Smolka, Modification of Mineral Powder by Various Organic Materials: Their Potential as Reinforcement for Unsaturated Polyester Composites, *Russ. J. Appl. Chem.*, 93, 2020, 1968-1975.